pH-controlled assembly of two new supramolecular hybrid compounds based on Keggin polyoxotungstates

Ya-Bing Liu, La-Mei Wang, Li-Na Xiao, Yang-Yang Hu, De-Chuan Zhao, Hai-Yang Guo, Peng Yu, Li-Wei Fu, Xiao-Bing Cui & Ji-Qing Xu

View supplementary material

Submit your article to this journal

View related articles

Citing articles: 2 View citing articles

Accepted author version posted online: 26 Nov 2014.
Published online: 22 Dec 2014.

Article views: 38

View Crossmark data

Taylor & Francis
Taylor & Francis Group

pH-controlled assembly of two new supramolecular hybrid compounds based on Keggin polyoxotungstates

YA-BING LIU†‡, LA-MEI WANG†, LI-NA XIAO†, YANG-YANG HU†,
DE-CHUAN ZHAO†, HAI-YANG GUO†, PENG YU§, LI-WEI FU†, XIAO-BING CUI†*
and JI-QING XU†

†Department of Chemistry, College of Chemistry and State Key Laboratory of Inorganic Synthesis
and Preparative Chemistry, Jilin University, Changchun, China
‡Department of Materials Science and Engineering, Jilin Jianzhu University, Changchun, China
§Department of Materials Science and Engineering, Jilin University, Changchun, China
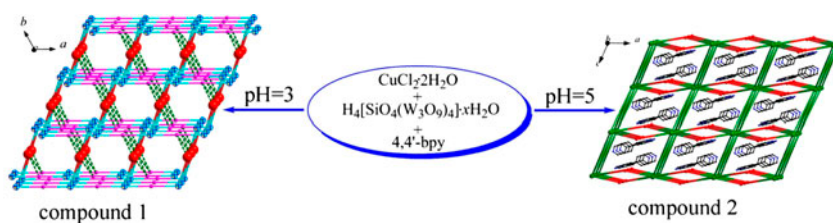
Two supramolecular compounds based on Keggin polyoxotungstates, (4,4′-H$_2$bpy){[Cu(4,4′-bpy)]$_2$[-SiW$_{12}$O$_{40}$]} (**1**) and (4,4′-H$_2$bpy)$_2$[SiW$_{12}$O$_{40}$]·2H$_2$O (**2**) have been synthesized and characterized by elemental analyses, IR, UV, XPS spectra, TG analyses, and single crystal X-ray diffraction analyses. Compound **1** exhibits an infinite 1-D ladder like structure, which is further interconnected into a 3-D supramolecular framework *via* hydrogen bonding interactions. Compound **2** contains 4,4′-bipyridine (4,4′-bpy), pseudo-Keggin polyoxoanions [SiW$_{12}$O$_{40}$]$^{4-}$, and water molecules. Polyoxoanions together with water molecules in **2** construct a 3-D inorganic supramolecular network through O···O and O···Ow(1) interactions. The electrochemical behaviors and photocatalytic properties of **1** and **2** have been investigated.

Keywords: Crystal structure; Hydrothermal synthesis; Keggin polyoxometalates; Hydrogen bonds; Photocatalytic property

1. Introduction

Directed assembly of supramolecular arrays from discrete molecular building blocks has increasing interest for potential applications in molecular electronics, sensor design, catalysis and optics in crystal engineering, and supramolecular chemistry [1–7]. In the

---

*Corresponding author. Email: cuixb@mail.jlu.edu.cn

construction of supramolecular materials, one important strategy is that low-dimensional building blocks extend to high-dimensional networks through weak intermolecular interactions, including hydrogen bonding, $\pi \cdots \pi$ stacking, and van der Waals interactions; hydrogen bonding is a dominant organizing force in supramolecular assemblies by virtue of its unique strength and directionality that may control short-range packing.

Because of their importance in nonlinear optical materials, medicines, and catalysis [8–18], Keggin polyoxometalates (POMs) have been employed as discrete building blocks accompanied with various moieties to construct supramolecular arrays because the spherical surface of POMs can give a better opportunity to form different kinds of hydrogen bonds [19–44]. The 4,4′-bpy is a rod-like moiety employed as a rigid building block for construction of coordination complexes based on POMs and transition metal complexes [28–30]. However, POMs directly combined with 4,4′-bpy for construction of supramolecular hybrids is less developed.

Our groups have recently reported some supramolecular materials based on POMs and 4,4′-bpy moieties [31–35]. In this article, we report the syntheses and characterizations of two new compounds constructed from 4,4′-bpy moieties and Keggin POMs: (4,4′-H_2bpy) $\{[Cu(4,4′-bpy)]_2[SiW_{12}O_{40}]\}$ (**1**) and (4,4′-H_2bpy)$_2$[SiW$_{12}$O$_{40}$]·2H$_2$O (**2**). Compound **1** presents an infinite 1-D ladder-like structure, which is further interconnected into a 3-D supramolecular framework *via* hydrogen bonding interactions. Compound **2** is based on 4,4′-bpy cations, pseudo-Keggin polyoxoanions $[SiW_{12}O_{40}]^{4-}$, and water molecules. Polyoxoanions together with water molecules construct an inorganic supramolecular network through complex O···O and O···Ow(1) interactions.

2. Experimental

2.1. *Materials and methods*

All chemicals were purchased and used without purification. Elemental analyses (C, H, and N) were performed on a Perkin-Elmer 2400 Series II CHNS/O elemental analyzer. Si, W, and Cu analyses were performed on a Perkin-Elmer Optima 3300DV spectrophotometer. IR spectra were obtained on a Perkin-Elmer spectrophotometer from 200 to 4000 cm^{-1} with pressed KBr pellets. UV spectra in DMSO solution were recorded on a Shimadzu UV-3100 spectrophotometer. XPS measurements were performed on a Thermo ESCALAS 250 spectrometer with an Mg-K$_\alpha$ (1253.6 eV) achromatic X-ray source. Thermogravimetric (TG) curves were performed on a Perkin-Elmer TGA-7000 thermogravimetric analyzer in flowing N$_2$ with a temperature rate of 10 °C min^{-1}.

2.2. *Syntheses*

2.2.1. Synthesis of (4,4′-H$_2$bpy)$\{[Cu(4,4′-bpy)]_2[SiW_{12}O_{40}]\}$ (1). H$_4$[SiO$_4$(W$_3$O$_9$)$_4$]·xH$_2$O (0.863 g, 0.3 mM), CuCl$_2$·2H$_2$O (0.034 g, 0.2 mM), 4,4′-bpy (0.079 g, 0.5 mM), and distilled water (20 mL) were mixed and stirred for 60 min, and pH of the mixture was adjusted to 5 with NH$_3$·H$_2$O. The mixture was transferred to a Teflon-lined autoclave (25 mL) and heated to 160 °C in 90 min, kept at that temperature for three days, and then cooled gradually to room temperature at 4 °C h^{-1}. Black block crystals of **1** suitable for X-ray diffraction

analysis were isolated in 72% yield (Based on W). Anal. Calcd for $C_{30}H_{26}N_6W_{12}Cu_2O_{40}Si$ (%): C, 10.38; H, 0.75; N, 2.42; W, 63.54; Cu, 3.66; Si, 0.81. Found: C, 10.33; H, 0.54; N, 2.48; W, 63.76; Si, 0.70.

2.2.2. Synthesis of $(4,4'\text{-}H_2bpy)_2[SiW_{12}O_{40}]\cdot2H_2O$ (2). Compound **2** was prepared with the identical procedure to that of **1**, with pH of the mixture adjusted to 3 instead of 5 with $NH_3\cdot H_2O$. Orange block crystals of **2** suitable for X-ray diffraction analysis were isolated in 65% yield (based on W). Anal. Calcd for $C_{20}H_{24}N_2W_{12}O_{42}Si$ (%): C, 7.45; H, 0.75; N, 1.74; W, 68.37; Si, 0.87. Found: C, 7.53; H, 0.72; N, 1.77; W, 68.51; Si, 0.63.

2.3. *X-ray crystallography*

Reflection intensity data for **1** and **2** were collected on a Rigaku R-AXIS RAPID IP diffractometer with graphite monochromated Mo-K_α ($\lambda = 0.71073$ Å) radiation. Neither crystal showed evidence of crystal decay during data collections. Both structures were solved by direct methods and refined using full-matrix least squares on F^2 with SHELXTL-97 crystallographic software. In final refinements, all atoms were refined anisotropically except the disordered 4,4′-bpy in **1** and water in **2**. Hydrogens were included in their ideal positions; those of the water and disordered 4,4′-bpy were not added. A summary of the crystallographic data and structure refinements for **1** and **2** is given in table 1. Selected bond lengths of **1** and **2** are listed in table S1 (see online supplemental material at http://dx.doi.org/10.1080/00958972.2014.991919).

Table 1. Crystal data and structure refinement parameters for **1** and **2**.

	1	2
Empirical formula	$C_{30}H_{26}Cu_2N_6O_{40}SiW_{12}$	$C_{20}H_{24}N_4O_{42}SiW_{12}$
Formula weight	3471.78	3226.55
Crystal system	Triclinic	Monoclinic
space group	*p-1*	*p21/c*
a (Å)	10.845(2)	11.550(1)
b (Å)	11.838(2)	12.092(1)
c (Å)	13.355(3)	18.459(2)
α (°)	104.33(3)	90
β (°)	103.07(3)	113.766(5)
γ (°)	114.98(3)	90
Volume (Å^3), Z	1395.0(5), 1	2359.5(18), 2
Calculated density D_c (mg/m^3)	4.133	4.542
Absorption coefficient (mm^{-1})	25.494	29.260
θ Range for data collection (°)	3.14–27.48	1.93–26.16
$F(0\,0\,0)$	1525	2819
Reflection collected	13,435/6278	12,451/4684
Goodness-of-fit on F^2	1.092	1.070
Final R indices [$I>2\theta(I)$]	[a]$R_1 = 0.0556$, [b]$wR_2 = 0.1480$	[a]$R_1 = 0.0861$, [b]$wR_2 = 0.1994$
Largest diff. peak and hole	2.875 and -3.444 eÅ^{-3}	4.423 and -4.340 eÅ^{-3}

[a]$R_1 = \sum||F_o| - |F_e||/\sum|F_o|$.
[b]$wR_2 = \{[\sum w(F_o^2 - F_e^2)^2]/[\sum w(F_o^2)^2]\}^{1/2}$.

3. Results and discussion

3.1. *Synthesis*

Compounds **1** and **2** were isolated from the reaction of $H_4[SiO_4(W_3O_9)_4] \cdot xH_2O$ and $CuCl_2 \cdot 2H_2O$ in the presence of 4,4′-bpy as structure-directing agent by the hydrothermal method with different pH values, as shown in scheme 1. The pH is crucial for formation of **1** and **2**. When pH is 5, **1** can be formed, and only at pH 3, was **2** formed. This shows that preparations of **1** and **2** need strictly controlled pH values of the reaction systems. If $CuCl_2 \cdot 2H_2O$ was substituted by $AgNO_3$, **3** can be synthesized [33]. The 4,4′-bpy also acts as a reducing agent under hydrothermal conditions, Cu^{II} in the starting materials of **1** was reduced in the presence of 4,4′-bpy.

3.2. *Crystal structure of 1*

Crystal structure analysis reveals that the asymmetric unit of **1** consists of a $[SiW_{12}O_{40}]^{4-}$, two $[Cu(4,4'\text{-bpy})]^+$ cations, and a disordered 4,4′-H_2bpy. As shown in figure 1, $[SiW_{12}O_{40}]^{4-}$ has a pseudo-Keggin structure [43] which is based on a central SiO_4^{4-} which exhibits cubic geometry with all eight oxygens half-occupied surrounded by four groups of internally edge-sharing tri-octahedral W_3O_{13}. Si–O distances vary from 1.562(2) to 1.684(2) Å. There are three kinds of oxygens in $[SiW_{12}O_{40}]^{4-}$: terminal (O_t) with W–O_t distances of 1.638(1)–1.704(1) Å, bridging (O_b) with W–O_b distances of 1.865(2)–1.940(2) Å, and central oxygens (O_c) with W–O_c distances of 2.325(2)–2.408(2) Å (table S1). Bond valence sum (BVS) calculations [45] for the six independent tungstens of **1** indicate that tungstens are in the +6 oxidation state [46].

There is only one crystallographically independent copper (Cu(1)) in **1**. Cu(1) has see–saw geometry with two nitrogens from two 4,4′-bpy ligands with Cu–N distances of 1.896(2)–1.907(2) Å, one terminal O(11) and one bridging O(5) from one neighboring $[SiW_{12}O_{40}]^{4-}$ with Cu–O distances of 2.623(2) and 2.727(1) Å. BVS calculations [45] for Cu(1) indicate that the oxidation state of Cu(1) is +1. Each 4,4′-bpy, acting as a bridge, links two Cu(1) ions, forming a 1-D $[Cu(4,4'\text{-bpy})]_n^{n+}$ chain. As illustrated in figure 2, the most unusual feature of **1** is that two neighboring $[Cu(4,4'\text{-bpy})]_n^{n+}$ chains are linked by $[SiW_{12}O_{40}]^{4-}$ clusters to build a ladder-like chain structure, in which $[SiW_{12}O_{40}]^{4-}$ clusters are bidentate inorganic ligands joining two neighboring chains. Each $[SiW_{12}O_{40}]^{4-}$ cluster is a ladder rung, and each $[Cu(4,4'\text{-bpy})]_n^{n+}$ chain serves as an edge of the ladder.
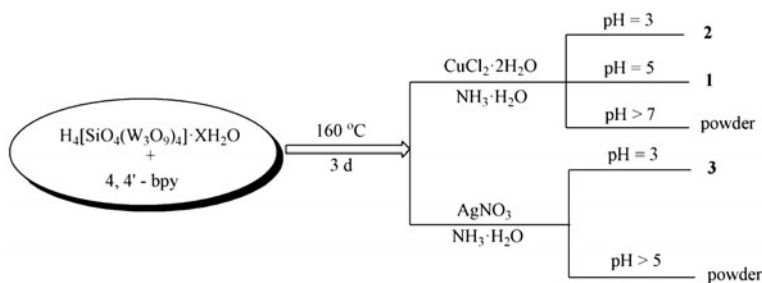
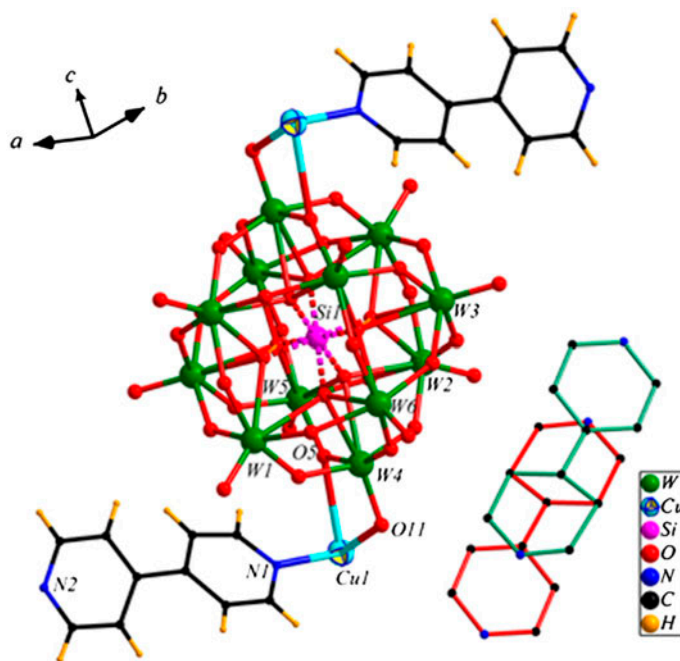Scheme 1. Experimental conditions for the synthesis of **1**, **2** and **3**.

Figure 1.   The building block of the pseudo-Keggin polyoxotungstate $(4,4'-H_2bpy)\{[Cu(4,4'-bpy)]_2 [SiW_{12}O_{40}]\}$.

Hydrogen bonds play important roles in stabilizing the crystal structure of **1**. As shown in figure 3, 1-D ladder like chains are linked to from a 2-D layer structure via C(2)–H···O (12) and its symmetry equivalent interactions with a C···O distance of 3.203(2) Å [figure 3(a)]. Two adjacent hydrogen-bonded layers (figure s1) are further connected through C(2)-H···O(16), C(3)–H···O(16) and their symmetry equivalent interactions with distances of 3.081(3)–3.217(3) Å, generating a 3-D supramolecular network [figure 3(b)]. Disordered bi-protonated $4,4'-H_2bpy$ cations are located in the holes of the 3-D supramolecular network. From another standpoint, each 1-D ladder like chain is linked with its four neighboring ones via hydrogen bonds into a 3-D supramolecular structure [see figure 3(c), table S1, and Supporting Information]. If the polyoxoanions, Cu ions, and 4,4′-bpy molecules that coordinate
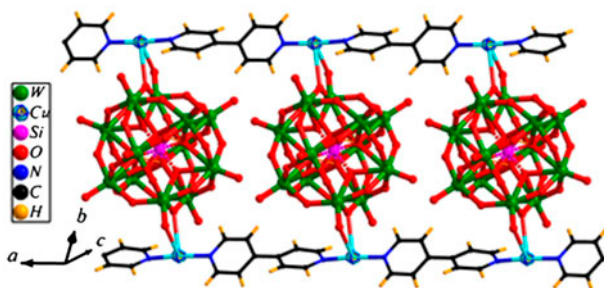

Figure 2.   Combined ball/stick representation of the 1-D rail-like structure of **1.**
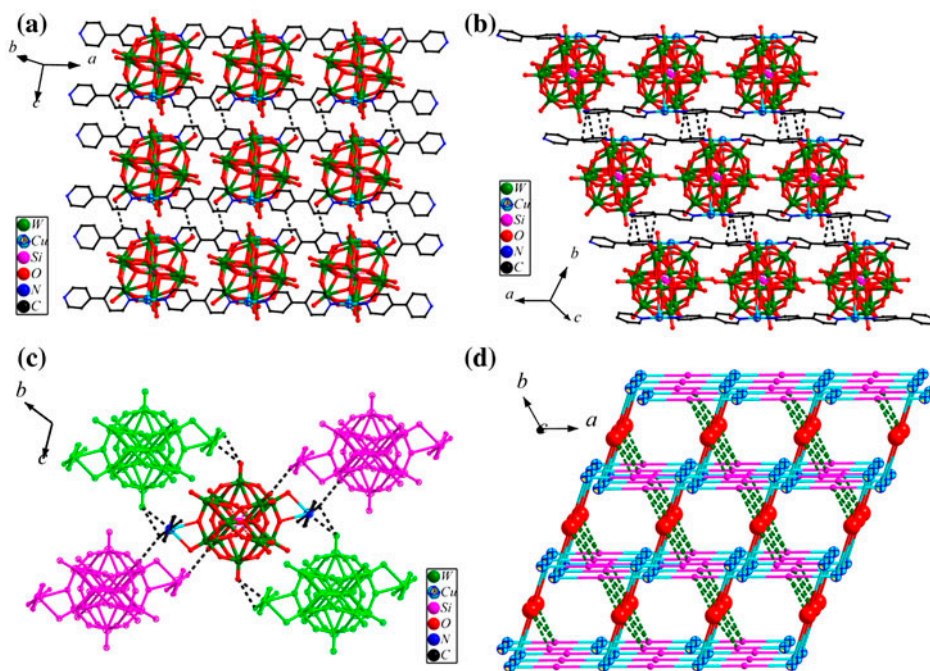
Figure 3. (a) View of the 2-D supramolecular layer structure with hydrogen bonding interactions between two neighboring 1-D chains. Several hydrogens are omitted for clarity. (b) View of the 3-D hydrogen-bonded framework of **1**. Some hydrogen bonds are omitted for clarity. (c) Combined ball/stick representation of $\{[Cu(4,4'-bpy)]_2[SiW_{12}O_{40}]\}^{2-}$ rail-like anion chain connected to four adjacent chains through C–H⋯O hydrogen bonding interactions on the *bc* plane. (d) Schematic drawing of the 3-D supramolecular topology in **1**.

to Cu(1) are perceived as nodes and hydrogen bonds as spacers, a 3-D topological structure can be obtained [shown in figure 3(d)].

Recently, some compounds constructed from copper complexes and Keggin $\{SiW_{12}O_{40}\}$ clusters have been reported [30, 47–49]. These compounds are all thoroughly different from compound **1** except for the compound reported by Peng *et al.* [30]. However, there exist significant differences between **1** and the Peng's compound. Firstly, the Keggin polyanion in Peng's compound is not $[SiW_{12}O_{40}]^{4-}$, but $[PMo_{12}O_{40}]^{3-}$. Secondly, also most importantly, there exists no similar disordered 4,4′-H_2bpy cations in Peng's compound (figure s2).

3.3. *Crystal structure of 2*

The asymmetric unit of **2** is composed of a Keggin polyanion $[SiW_{12}O_{40}]^{4-}$, two bi-protonated 4,4′-H_2bpy moieties, and two water molecules (figure s3). Bond valence sum (BVS) calculations for the six independent tungsten ions of **2** indicate that the tungsten atoms are in the +6 oxidation state.

As illustrated in figure 4, each $[SiW_{12}O_{40}]^{4-}$ is linked to four adjacent ones through four O⋯O interactions to form a 2-D inorganic supramolecular layer; O⋯O distances are 3.088 (5)–3.068(3) Å. These distances between oxygens are in the range of distances of general O–H⋯O hydrogen bonds. Adjacent 2-D inorganic layers are further connected through O–H⋯O hydrogen bonding interactions between oxygens of water and polyanions with
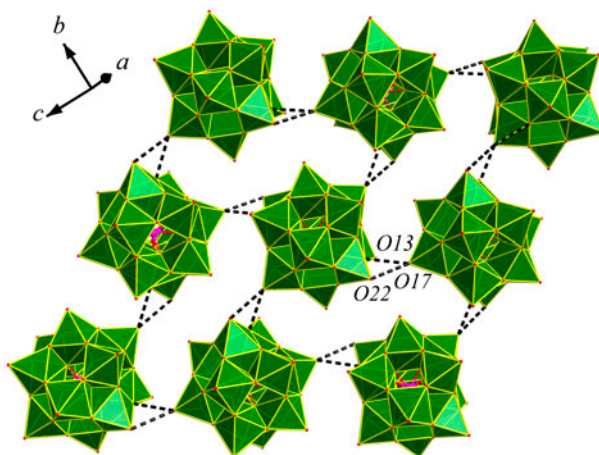
Figure 4.   View of the 2-D supramolecular layer structure of **2** constructed from O···O interactions among POMs. The 4,4′-bpy cations and water molecules have been omitted for clarity.

O···O distances of 3.028(5)–3.153(4) Å (figure s4), generating an interesting 3-D inorganic supramolecular network.

The schematic representation of the 3-D networks of **2** constructed from POMs and Ow(1) through O–H···O interactions is depicted in figure 5. Each $[SiW_{12}O_{40}]^{4-}$, as a node, connects four adjacent $[SiW_{12}O_{40}]^{4-}$ anions and four adjacent Ow(1). Alternately, each Ow(1) links two adjacent $[SiW_{12}O_{40}]^{4-}$ anions. Therefore, POMs and Ow(1) water molecules assemble into a 3-D supramolecular network through complex O···O and O···Ow(1) interactions [figure 5(a)]. Further analysis of **2** reveals that the cavities of the 3-D network are occupied by 4,4′-bpy cations. Each 4,4′-H₂bpy connects six POMs and one water via N–H···O and C–H···O hydrogen bonding interactions with N···O and C···O distances of 2.836(6)–3.012(1) Å and 3.173(5)–3.203(3) Å, respectively. Selected hydrogen bonds are listed in table 2.

3.4. *Characterization of the compounds*

3.4.1. IR spectra. IR spectra of **1** and **2** are shown in figure s5 (Supporting Information). Characteristic bands at 979, 922, 880, and 792 cm^{-1} for **1** and 976, 922, 882, and 792 cm^{-1} for **2** are attributed to v(W–O$_t$), v(Si–O), v(W–O$_b$–W), and v(W–O$_c$–W), respectively [50]. Bands at 1221–1628 cm^{-1} for **1** and 1211–1610 cm^{-1} for **2** are due to vibrations of 4,4′-bpy.

3.4.2. UV–Vis spectroscopy. The UV–Vis spectra of **1** and **2**, in the range of 250–400 nm, are presented in figure s6. Characteristic bands at 261.9 nm for **1** and 262.4 nm for **2** are attributed to O → W charge transfer band in the polyanion of **1** and **2** [51]. Spectra for **1** and **2** are very similar to each other, indicating that **1** and **2** contain similar Keggin-type POMs.

3.4.3. XPS spectra. Figure s7(a) shows the XPS spectrum of **1** with two overlapped peaks at 37.8 and 35.7 eV, respectively, ascribed to W^{6+} 4f$_{5/2}$ and W^{6+} 4f$_{7/2}$. The XPS spectrum of
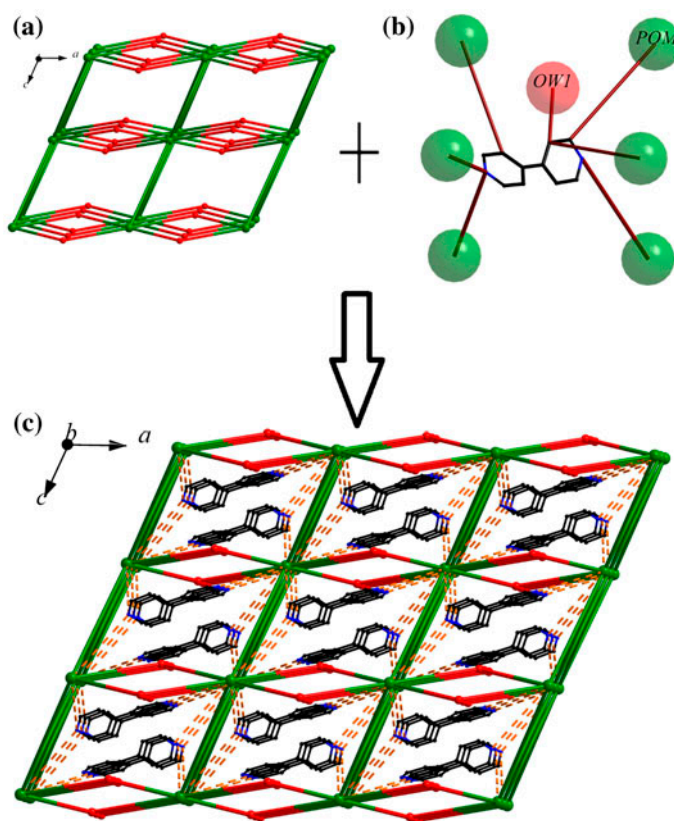
Figure 5. (a) Schematic view of the 3-D network of **2** (POM, green; water molecule, red). (b) Combined ball/stick representation of 4,4′-bpy connecting six neighboring POMs and one water molecule through C–H⋯O and N–H⋯O hydrogen bonding interactions. Hydrogens are omitted for clarity. (c) Schematic representation of the host–guest assembly in **2**. Several C–H⋯O and N–H⋯O hydrogen bonds are omitted for clarity (see http://dx.doi.org/10.1080/00958972.2014.991919 for color version).

2 gives two peaks at 38.1 and 36.0 eV attributed to W^{6+} $4f_{5/2}$ and W^{6+} $4f_{7/2}$ [Figure s7(b)], respectively. The XPS estimation of valence is in reasonable agreement with those calculated from bond valence sum calculations.

3.4.4. Thermogravimetric analysis. The TG analysis curves of **1** and **2** are shown in figure s8. The curve of **1** shows a total weight loss of 13.36% from room temperature to 480 °C, which corresponds to the release of 4,4′-bpy moieties (calcd. 13.55%). The TG curve of **2** can be divided into two stages. The first weight loss is 1.06% from room temperature to 167 °C, ascribed to release of water molecules (calcd. 1.12%). The second weight loss is 10.19% from 343 to 456 °C, attributed to the decomposition of 4,4′-bpy moieties in **2** (calcd. 9.81%).

3.4.5. Cyclic voltammetry. Cyclic voltammograms of DMSO solutions of **1** and **2** in 1 M L^{-1} H_2SO_4 at 100 mV s^{-1} are presented. For **1**, as shown in figure s9(a), at potentials

Table 2. Hydrogen bond parameters for **1** and **2**.

	D–H···A (Å)		D–H···A (Å)
Compound **1**			
C2–HO12	3.203(2)	C3–H···O16(#1)	3.217(3)
C2–H···O16(#1)	3.081(3)	C7–H···O5(#2)	3.080(4)
N2–H···O5(#2)	3.106(3)	N2–H···O11(#2)	3.265(3)
Compound **2**			
N1–H···O12(#1)	2.836(6)	N1–H···O9(#2)	3.012(6)
N2–H···O21(#3)	2.867(3)	N2–H···O22	3.084(5)
N2–H···O17(#4)	3.136(4)	C1–H···O10(#2)	3.160(7)
C1–H···O19(#1)	3.177(6)	C2–H···O8(#2)	3.194(5)
C3–H…..O8(#2)	3.190(4)	C3–H···O20(#4)	3.203(3)
C6–H···O21(#3)	3.136(5)	C6–H···O15(#5)	3.259(4)
C7–H···O22	3.183(6)	C8–H···O20(#4)	3.288(5)
C9–H···O15(#6)	3.258(5)	C9–H···O22(#2)	3.244(5)
C9–H···O16(#2)	3.268(4)	C10–H···O15(#6)	3.160(5)
C10–H···O16(#2)	3.138(5)	OW1···O14(#7)	3.102(4)
OW1···O11	3.028(5)	C8···OW1(#2)	3.173(5)
OW1···O19(#6)	3.153(4)	C7···OW1(#8)	3.056(5)

Notes: Symmetric components for **1** #1: $x, y, -1 + z$; #2: $2 - x, 1 - y, 1 - z$.
Symmetric components for **2** #1: $-1 + x, -0.5 - y, 0.5 + z$; #2: $1 - x, -y, 1 - z$; #3: $2 - x, -y, 1 - z$; #4: $x, -0.5 - y, 0.5 + z$; #5: $2 - x, 0.5 + y, 1.5 - z$; #6: $-1 + x, y, z$; #7: $2 - x, -1 - y, 1 - z$; #8: $1 - x, -1 - y, 1 - z$.

of −100 to −700 mV, there exist three reversible redox peaks I–I′, II–II′, and III–III′ with half-wave potentials $E_{1/2} = (E_{pa} + E_{pc})/2$ at −605, −492, and −341 mV, respectively. The three redox peaks correspond to one two-electron and two consecutive one-electron processes of W [52]. For **2**, as shown in figure s9(b), at potentials of −100 to −700 mV, there exist three reversible redox peaks I–I′, II–II′, and III–III′ with half-wave potentials $E_{1/2} = (E_{pa} + E_{pc})/2$ at −559.5, −492.5, and −338.5 mV, respectively. The three redox peaks correspond to one two-electron and two consecutive one-electron processes of W.

3.4.6. Photocatalytic property. In a typical process, 5 mg (0.0014 mM) **1** or 4.65 mg (0.0014 mM) **2** were ground for about 10 min with an agate mortar to obtain a fine powder, and then the powder was dispersed in 100 mL rhodamine B (RhB) solutions (1.0×10^{-5} M L^{-1}). The suspension was agitated in an ultrasonic bath for 20 min in the dark and
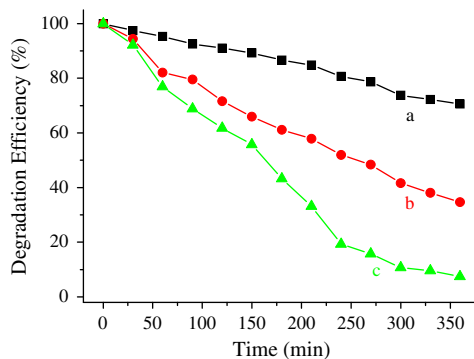

Figure 6. Photocatalytic activities of **1** and **2** for the degradation of RhB (1×10^{-5} M L^{-1}, 100 mL) under UV light. (a) Without any catalyst, (b) **1**, and (c) **2**.

then, magnetically stirred in the dark for about 30 min. The suspension was finally exposed to UV irradiation from a 300 W Hg lamp at a distance of 4–5 cm between the liquid surface and the lamp. The suspension was stirred during irradiation at a stirring rate of 790–800 rpm. At 30 min intervals, 5 mL samples were taken from the beaker, which were clarified by centrifugation at 10,000 rpm for 5 min, and subsequently analyzed by UV–visible spectroscopy (figure s10). The photodegradation process of RhB without any photocatalyst has been studied for comparison, and only 29% of RhB was photodegraded after 360 min. Changes in C_t/C_0 plot of RhB solutions *versus* reaction time are shown in figure 6. Compared with RhB without any photocatalyst, the absorption peaks of **1** and **2** decreased obviously upon irradiation, indicating that these compounds have excellent photocatalysis properties for photocatalytic degradation of RhB.

The photocatalytic properties of **1** and **2** are shown in figure 6. The conversions of RhB are 65.31% for **1** and 92.57% for **2**, indicating that both compounds may be good candidates for photocatalysts in the reduction of organic dyes.

4. Conclusion

Two new hydrogen-bonded supramolecular compounds have been isolated by hydrothermal methods and structurally characterized. Compound **1** exhibits an infinite rail-like chain structure. The most striking feature of **2** is that water molecules link adjacent polyanions into a 3-D inorganic supramolecular network through hydrogen bonds.

Supplementary material

CCDC reference numbers: 980624 for **1** and 980625 for **2**. These data can be obtained free of charge from the Cambridge Crystallographic Data Center via www.ccdc.cam.ac.uk/data_request/cif.

Funding

References

[1] J.M. Lehn. *Supramolecular Chemistry*, VCH, New York, NY (1995).
[2] F. Vögtle. *Supramolecular Chemistry*, Wiley, Chicester (1991).
[3] M. Lehn. *Comprehensive Supramolecular Chemistry*, Pergamum, New York, NY (1996).
[4] J.M. Lehn. *Angew. Chem. Int. Ed. Engl.*, **29**, 1304 (1990).
[5] C.N.R. Rao, S. Natarajan, R. Vaidhyanathan. *Angew. Chem. Int. Ed. Engl.*, **43**, 1466 (2004).
[6] O.M. Yaghi, M. O'Keeffe, N.W. Ockwig, H.K. Chae, M. Eddaoudi, J. Kim. *Nature*, **423**, 705 (2003).
[7] J.L.C. Rowsell, O.M. Yaghi. *Microporous Mesoporous Mater*, **73**, 3 (2004).
[8] S.V. Kolotuchin, E.E. Fenlon, S.R. Wilson, C.J. Loweth, S.C. Zimmerman. *Angew. Chem. Int. Ed.*, **34**, 2654 (1995).
[9] J.M. Lehn. *Science*, **295**, 2400 (2002).
[10] B.J. Holliday, C.A. Mirkin. *Angew. Chem. Int. Ed.*, **40**, 2022 (2001).

[11] K. Biradha, Y. Hongo, M. Fujita. *Angew. Chem. Int. Ed.*, **39**, 3843 (2000).
[12] M. Eddaoudi, D.B. Moler, H. Li, B. Chen, T.M. Reineke, M. O'Keeffe, O.M. Yaghi. *Acc. Chem. Res.*, **34**, 319 (2001).
[13] A.X. Tian, X.L. Lin, Y.J. Liu, G.Y. Liu, J. Ying, X.L. Wang, H.Y. Lin. *J. Coord. Chem.*, **65**, 2417 (2012).
[14] M.L. Wei, H.H. Li, G.J. He. *J. Coord. Chem.*, **65**, 4318 (2012).
[15] M.T. Pope. *Heteropoly and Ispoly Oxometalates*, Spring-Verlag, Berlin (1983).
[16] C. Hill. *Chem. Rev.*, **98**, 1 (1998).
[17] A. Müller, M. Koop, P. Schiffels, H. Bögge. *Chem. Commun.*, **18**, 1715 (1997).
[18] D.L. Long, R. Tsunashima, L. Cronin. *Angew. Chem. Int. Ed. Engl.*, **49**, 1736 (2010).
[19] Y. Xu, H.G. Zhu, H. Cai, X.Z. You. *Chem. Commun.*, **9**, 787 (1999).
[20] E. Burkholder, J. Zubieta. *Chem. Commun.*, **20**, 2056 (2001).
[21] M.L. Khan, S. Cevik, R. Hayashi. *J. Chem. Soc. Dalton Trans.*, 2879 (2002).
[22] C. Streb, D.L. Long, L. Cronin. *CrystEngComm*, **8**, 629 (2006).
[23] D.P. Cheng, M.A. Khan, R.P. Houser. *Inorg. Chem.*, **40**, 6858 (2001).
[24] D.F. Sun, R. Cao, Y.Q. Sun, W.H. Bi, X.J. Li, Y.Q. Wang, Q. Shi, X. Li. *Inorg. Chem.*, **42**, 7512 (2003).
[25] H. Kumagai, M. Arishima, S. Kitagawa, K. Ymada, S. Kawata, S. Kaizaki. *Inorg. Chem.*, **41**, 1989 (2002).
[26] J. Miao, S.X. Zhang, S.J. Li, Y.H. Gao, X. Zhang, X.N. Wang, S.X. Liu. *J. Coord. Chem.*, **64**, 4006 (2011).
[27] J. Miao, Y.W. Liu, Q. Tang, D.F. He, G.C. Yang, Z. Shi, S.X. Liu, Q.Y. Wu. *J. Chem. Soc. Dalton Trans.*, 14749 (2014).
[28] F. Yao, F.X. Meng, Y.G. Chen, C.J. Zhang. *J. Coord. Chem.*, **63**, 196 (2010).
[29] C.M. Wang, S.T. Zheng, G.Y. Yang. *J. Cluster Sci.*, **20**, 489 (2009).
[30] J.Q. Sha, J. Peng, Y. Zhang, H.J. Pang, A.X. Tian, P.P. Zhang. *Cryst. Growth Des.*, **9**, 1708 (2009).
[31] Z.H. Yi, X.B. Cui, X. Zhang, G.D. Yang, J.Q. Xu, X.Y. Yu, H.H. Yu, W.J. Duan. *J. Mol. Struct.*, **891**, 123 (2008).
[32] Y. Wang, F.Q. Wu, L. Ye, T.G. Wang, G.W. Wang, S.Y. Shi, L.N. Xiao, X.B. Cui, J.Q. Xu. *Inorg. Chem. Commun.*, **13**, 703 (2010).
[33] Y.B. Liu, Y. Wang, L.N. Xiao, Y.Y. Hu, L.M. Wang, X.B. Cui, J.Q. Xu. *J. Coord. Chem.*, **65**, 4243 (2012).
[34] L.N. Xiao, Y. Wang, Y. Peng, G.H. Li, J.N. Xu, L.M. Wang, Y.Y. Hu, T.G. Wang, Z.M. Gao, D.F. Zheng, X.B. Cui, J.Q. Xu. *Inorg. Chim. Acta*, **204**, 387 (2012).
[35] Y. Wang, L. Ye, H. Ding, T.G. Wang, G.W. Wang, S.Y. Shi, X.B. Cui, J.Q. Xu. *J. Coord. Chem.*, **63**, 426 (2010).
[36] S. Noro, S. Kitagawa, M. Kondo, K. Seki. *Angew. Chem. Int. Ed.*, **39**, 2082 (2000).
[37] L.G. Zhu, S. Kitagawa. *Inorg. Chem. Commun.*, **6**, 1051 (2003).
[38] A.S. Attia, C.G. Pierpont. *Inorg. Chem.*, **34**, 1172 (1995).
[39] H.J. Chen, L.Z. Zhang, Z.G. Cai, G. Yang, X.M. Chen. *J. Chem. Soc. Dalton Trans.*, 2463 (2000).
[40] H.X. Yang, X. Lin, B. Xu, M.N. Cao, S.Y. Cao, R. Cao. *J. Mol. Struct.*, **33**, 966 (2010).
[41] J.Q. Sha, J. Peng, H.J. Pang, A.X. Tian, J. Chen, P.P. Zhang, M. Zhu. *Solid State Sci.*, **10**, 1419 (2008).
[42] F.X. Ma, Q. Zhao. *Acta Crystallogr. Sect. E*, **64**, 1224 (2008).
[43] M.A. Porai-Koshits, V.S. Sergienko, E′.N. Yurchenko. *J. Struct. Chem.*, **27**, 176 (1986).
[44] H.J. Pang, J. Peng, J.Q. Sha, A.X. Tian, P.P. Zhang, Y. Chen, M. Zhu. *J. Mol. Struct.*, **922**, 88 (2009).
[45] D. Altermatt, I.D. Brown. *Acta Crystallogr. B*, **41**, 240 (1985).
[46] N. Gharah, K. Chowdhury, M. Mukherjee, R. Bhattacharyya. *Transition Met. Chem.*, **33**, 635 (2008).
[47] J. Wu, Y.L. Xu, K. Yu, Z.H. Su, B.B. Zhou. *J. Coord. Chem.*, **66**, 2821 (2013).
[48] S.H. Yang, X.Q. Dong, Y.P. Zhang, H.M. Hu, G.L. Xue. *J. Coord. Chem.*, **66**, 1529 (2013).
[49] W.Q. Kan, J.M. Xu, Y.H. Kan, Jiao Guo. *J. Coord. Chem.*, **67**, 195 (2014).
[50] J.Q. Sha, J.W. Sun, C. Wang, G.M. Li, P.F. Yan, M.T. Li. *Cryst. Growth Des.*, **12**, 2242 (2012).
[51] Q.G. Zhai, X.Y. Wu, S.M. Chen, Z.G. Zhao, C.Z. Lu. *Inorg. Chem.*, **46**, 5046 (2007).
[52] M.G. Liu, P.P. Zhang, J. Peng, H.X. Meng, X. Wang, M. Zhu, D.D. Wang, C.L. Meng, K. Alimaje. *Cryst. Growth Des.*, **12**, 1273 (2012).